Haifeng DAI, Xuezhe WEI, Zechang SUN

Tongji University

Design and Implementation of a UKF-based SOC Estimator for LiMnO2 Batteries Used on Electric Vehicles

Abstract. *To ensure safe and reliable battery operations, an accurate battery state of charge (SOC) estimation is critical for the battery systems used in electric vehicles and hybrid electric vehicles because of the arduous operation conditions. This paper presents a SOC estimator designed based on the unscented Kalman filter (UKF), which is very popular in the state estimation in non-linear systems. The dynamic characteristics of the battery are modeled with an equivalent circuit, which is composed of two capacitors, three resistors and a voltage source to simulate the equilibrium open circuit voltage (OCV). To relieve the computation requirement of the original UKF, an efficient implementation using a Cholesky factorization is investigated, and thereby a SR-UKF based SOC estimator is proposed. Experiment results shows that the model proposed can track the dynamic behavior of the battery very well and the UKF-based SOC estimator has a good performance in the state estimation, and a comparison with EKF-based estimator also shows that a better accuracy can be got by the proposed UKF- based estimator.*

Streszczenie. *Artykuł prezentuje system kontroli SOC (state of charge – stan naładowania) baterii używanych w pojazdach elektrycznych. System bazuje na filtrze Kalmana typu UKF. Własności dynamiczne baterii modelowane są przy pomocy odpowiedniego obwodu elektrycznego zastępczego. System może śledzić właściwości dynamiczne baterii i badać jej stan naładowania. (**Projekt i zastosowanie estymatora stanu naładowania baterii LiMnO2 używanych w pojazdach elektrycznych**)*

Keywords: Electric Vehicles; Unscented KalmanFilter; State of Charge; Battery Modeling.
Słowa kluczowe: pojazdy elektryczne, stan naładowania, właściwości dynamiczne, filtr Kalmana

Introduction

Energy storage and environmental destruction have become the most important global issues in recent years, essentially raising more requirements on vehicle engineering. In order to reduce waste gas emission and reproduce energy in driving process, some new energy vehicles have been proposed to replace the traditional vehicles driven by gasoline, such as electric vehicle (EV) and hybrid electric vehicle (HEV). EVs and HEVs potentially can take advantage of renewable electricity sources, reduce reliance on fossil fuels, and are widely viewed as an important transitional technology towards sustainable transportation.

Traction battery pack, which is a critical sub-system of EVs/HEVs, is currently both performance and cost bottlenecks of EVs/HEVS. Since the early 1990s, lithium-ion batteries state a key technology in rechargeable batteries due to their high volumetric and gravimetric energy densities and are widely used in personal devices like camcorders, cellular phones and mobile computers today. Ongoing evolutionary advances released a new spate of intensive research activities to extend the operational area of small-sized batteries with the final aim to achieve reliable energy storage in automotive environments like EVs and HEVs. The high absolute energy content of large scale lithium-ion batteries however also raises safety and lifetime issues.

Due to the transient and demanding vehicle operations in daily driving, which mainly act as large dynamic transients in current and power demand over a wide temperature range, a battery management system (BMS) is required to ensure safe and reliable battery operations. The BMS needs to provide accurate knowledge of the states of the traction battery pack to operate the battery reliably and efficiently. One of the most important states of the battery pack is state of charge (SOC). To accommodate the operation conditions, the BMS should 'know' SOC to facilitate safe and efficient utilization of the battery pack, by preventing under- or over- charging conditions, thereby extending the lifetime and preventing progressive permanent damage to the battery.

An assortment of techniques have previously been reported to measure or estimate the SOC of the cells or battery pack, each having its relative merits, as reviewed by Piller et al [1]. Considering the working conditions of the battery packs on EVs/HEVs, the most commonly used strategy is the coulomb counting, or current integration techniques, requiring accurate measurements of the pack's current. Due to the open-loop calculation and integration, this strategy relies on the accuracy of the current measurement, errors in terminal measurement due to noise, resolution and rounding are cumulative, and large SOC errors can result. Other factors that ultimately influence the accuracy in SOC estimations are the variation of cell pack capacity with discharge rate, temperature and Coulombic efficiency losses. To recalibrate the SOC estimated by using coulomb counting, a method combining coulomb counting and equilibrium open circuit voltage (OCV) is recruited, since OCV varies over the whole range of SOC. In this method, the measured OCV is used to periodically correct the SOC derived from coulomb counting. However, suitable operational conditions for OCV measurement may not occur frequently enough in HEV driving duties for this to be successfully utilized.

Other reported methods for estimating SOC used on HEV's battery pack have been based on artificial neural networks (NN) and fuzzy logic principles, although the latter was reported to have relative poor performance. Such techniques incur large computation overhead on the BMS, which could lead to problems for online implementation and may increase the device cost. However, neural networks have been used to avoid the need for the large number of empirically derived parameters required by other methods. Indeed, for applications to less demanding task of prediction of SOC in portable equipment, a neural network modeling approach has been shown to give mean errors of about 3% [2]. Also, a neural network model for predicting battery power capacity during cycles has been added to ADVISOR EV and HEV modeling environments [3]. Other researches using NN-based estimators could also be seen in [4-10]. Research shows that the SOC estimator built based on NN can provide good SOC estimates, given an appropriate training data set, due to the powerful capability of computational intelligence to approximate non-linear function surfaces. Salkind et al. [11] utilized the fuzzy logic to implement the SOC estimation for lithium-ion batteries, on the basis of the training datasets got by impendence spectroscopy (EIS) and coulomb counting techniques.

Adaptive neural-fuzzy inference systems have also been investigated in [12, 13] for predicting the available capacity for nickel-metal and lithium-ion batteries. At the same time, support vector regression has also been used to estimate the battery SOC. A support vector based battery SOC estimator has been developed for large-scale lithium-ion battery packs in [14, 15]. Hu el al. [16] used a fuzzy clustering based support vector regression algorithm to build a SOC estimator for lithium-ion batteries for EVs.

Recent research shows that the Kalman filter based techniques has been popular in the design of SOC estimator. Gregory L. Plett [17, 18] has proposed a technique based on extended Kalman filter (EKF) to predict the SOC of the lithium-ion battery for HEVs, however, the model he applied to get a high accuracy is some complicated and without a specific physical meaning, which led to an intricate system identification directly. Dai el al. [19, 20] also proposed an EKF based SOC estimator which recruits an equivalent circuit as battery model, and achieved a good performance. Anyway, the EKF based methods has some shortcomings. For example, linearization would cause highly unstable filters if the assumption of local linearity matrices is nontrivial and error-prone. As an alternative approach to state estimation for non-linear systems, sigma-point Kalman filter (SPKF) has a higher order of accuracy in estimating the mean and the error covariance of the state vector than EKF. The two most common SPKF-based methods are central difference Kalman filter (CDKF) and unscented Kalman filter (UKF). A CDKF based on a nonlinear enhanced self-correcting (ESC) battery model has been studied in [21] for the SOC estimation of a LiPB battery, demonstrating a better accuracy than EKF-based estimator. UKF based on a non-linear electro-chemical battery model has been investigated in [22] for estimating the SOC of a lithium-ion cell. In [23], a zero-state hysteresis battery model based UKF SOC estimator was proposed.

In this paper, based on an equivalent circuit battery model, a UKF –based SOC estimator is developed to online estimate the SOC of a lithium-ion battery for EVs/HEVs. Considering the computation cost, the model is simplified to an equivalent circuit including 3 resistors, 2 capacitors and a voltage source. Battery cells tested in this paper are LiMnO2-based. The remainder of this paper is organized as follows. A description of the structure and parameterization of the equivalent circuit based battery model is given in section 2. The UKF -based SOC estimator is depicted in Section 3. Testing results with UKF -based SOC estimation approach is illustrated in Section 4. Finally, Conclusions are drawn in Section 5.

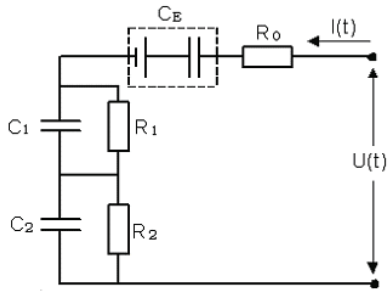

Fig.1. Equivalent Circuit model of Battery

Battery Modeling

Model Structure

Paper [24] reviewed several kinds of battery models used on EVs/HEVs currently. Here, a dynamic model of the lithium-ion battery pack, Fig.1, shows a simplified equivalent circuit accredit to Dr. Wei [25]. This model recuits R_0 as the internal ohmic resistance and C_E as open circuit voltage of the cell respectively. The R_1C_1 and R_2C_2 circuits simulate the delay or hysteresis of the battery terminal voltage between charging and discharging caused by the polarization and other factors. Note that, C_E here is not a pure capacitor, instead, it is used to decide the OCV of the pack according to the relationship between SOC and OCV as shown in Fig.2. From Fig.2, we can find that the relationship between SOC and OCV is obviously nonlinear.

Referring to [8-9], the states of the model are set to be SOC, $U^{R_1C_1}$ and $U^{R_2C_2}$, input of the model is current I, output is terminal voltage U, then, state vector $\boldsymbol{x} = (SOC, U^{R_1C_1}, U^{R_2C_2})'$. Voltage on C_E, $U^{R_1C_1}$ is the sum of the zero-state response and the zero-input response of R_1C_1 circuit to current I, and $U^{R_2C_2}$ is the sum of the zero-state response and the zero-input response of R_2C_2 circuit to current I.

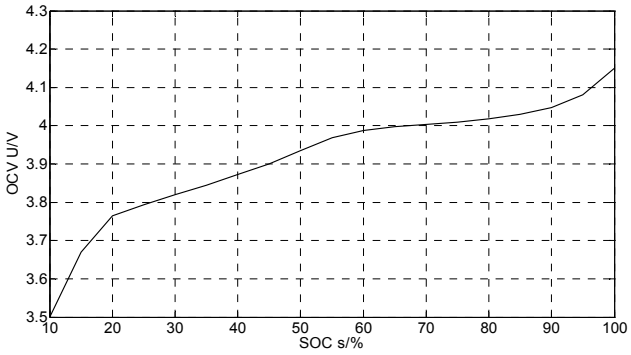

Fig.2. OCV variation of SOC

So the dynamic equivalent circuit model could be described in non-linear state-space as

$$\begin{pmatrix} SOC_{k+1} \\ U_{k+1}^{R_1C_1} \\ U_{k+1}^{R_2C_2} \end{pmatrix} = \begin{pmatrix} 1 & 0 & 0 \\ 0 & e^{-\Delta t/\tau_1} & 0 \\ 0 & 0 & e^{-\Delta t/\tau 2} \end{pmatrix} \times \begin{pmatrix} SOC_k \\ U_k^{R_1C_1} \\ U_k^{R_2C_2} \end{pmatrix} + \begin{pmatrix} -\frac{\eta_i \Delta t}{C} \\ R_1(1-e^{-\Delta t/\tau_1}) \\ R_2(1-e^{-\Delta t/\tau 2}) \end{pmatrix} i_k \quad (1)$$

$$U_k = OCV(SOC_k) - i_k R_0 - U_k^{R_1C_1} - U_k^{R_2C_2} \quad (2)$$

where Δt is the sample period of current and voltage, η_i is the Coulombic efficiency, usually, $\eta_i = 1$ when discharging and $\eta_i < 1$ when charging, η could be got by experiment. τ_1 and τ_2 are the time constant of the R_1C_1 and R_2C_2 circuit respectively, and $\tau_1 = R_1C_1$, $\tau_2 = R_2C_2$.

Model Parameterization

During aging process of the battery, parameters in this model would change. To accommodate this, parameters in this model could be identified each time when starting the vehicle. Given the sampled current, voltage, the parameter

vector of the battery model can be solved using the least squares (LS) algorithm. And the principle is described as shown in Fig.3 [25].

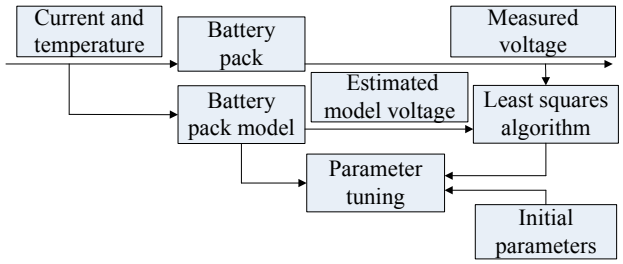

Fig.3. Model parameterization by using LS

Model Validation

The validity of the proposed model is undertaken by subjecting both the battery cell and the model to a current series, Fig. 4, which is sampled when the vehicle tested under J1015 cycles, for a comparison of the modeled voltage to the measured cell voltage, as shown in Fig.5. The time step is 20ms in this test.

With the equivalent circuit based model structure and a LS based parameter identification procedure, the battery model performs well under the test. We can find in Fig.5 that, even if under a very arduous current profile, the model could track the dynamic characteristics of the battery very well, although there is some error between the true voltage and the modeled voltage, the maximum error is less than 0.6%.

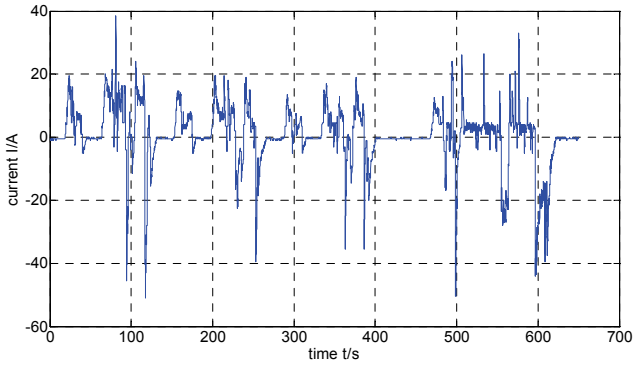

Fig.4. Current profile under J1015 cycle

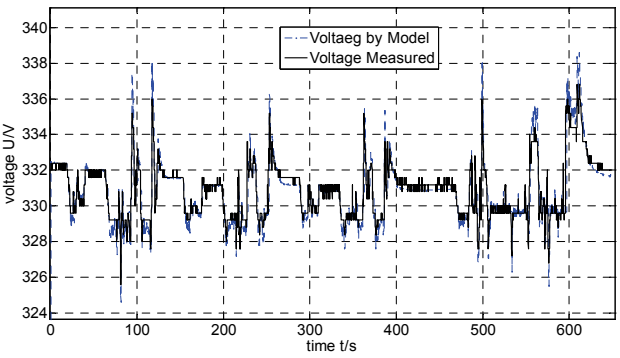

Fig.5. Voltage variation under J1015 cycle

The SOC Estimator Based on UKF

The Unscented Kalman Filter

Although the EKF has been used in the SOC estimation for batteries, the inherent flaws of the EKF are due to its linearization approach for calculating the mean and covariance of a random variable which undergoes a nonlinear transformation. The UKF [26-27], instead, addresses these flaws by utilizing a deterministic "sampling" approach to calculate mean and covariance terms. Essentially, 2L+1 sigma points (L is the state dimension), are chosen based on a square-root decomposition of the prior covariance. These sigma points are propagated through the true nonlinearity, without approximation, and then a weighted mean and covariance is taken.

The full UKF involves the recursive application of this "sampling" approach to the state-space equations. The traditional UKF implementation is given in Table 1 for state-estimation, and uses the following variable definition: $\{W_i\}$ is a set of scalar weights

($W_0^{(m)} = \lambda/(L+\lambda)$, $W_0^{(c)} = \lambda/(L+\lambda)+(1-\alpha^2+\beta)$, $W_i^{(m)} = W_i^{(c)} = 1/\{2(L+\lambda)\}$, $i=1,...,2L$). $\lambda = L(\alpha^2-1)$

and $\eta = \sqrt{L+\lambda}$ are scaling parameters. The constant α determines the spread of the sigma points around $\hat{\mathbf{x}}$ and is usually set to be $1e-4 \le \alpha \le 1$. β is used to incorporate prior knowledge of the distribution of $\mathbf{x}$ (for Gaussian distribution, $\beta = 2$ is optimal).

Table 1. Summary of the UKF Algorithm

Initialization:

$$k = 0$$

$$\hat{\boldsymbol{x}}_0^+ = \mathrm{E}(\boldsymbol{x}_0)$$

$$\boldsymbol{P}_0 = \boldsymbol{\Sigma}_{x_0}^+ = \mathrm{E}[(\boldsymbol{x}_0 - \hat{\boldsymbol{x}}_0^+)(\boldsymbol{x}_0 - \hat{\boldsymbol{x}}_0^+)^T]$$

$$\hat{\boldsymbol{x}}_{ex,0}^+ = \mathrm{E}(\boldsymbol{x}_{ex,0}) = \left[\hat{\boldsymbol{x}}_0^+, \quad 0, \quad 0\right]$$

$$\boldsymbol{P}_{ex,0} = \mathrm{E}[(\boldsymbol{x}_{ex,0} - \hat{\boldsymbol{x}}_{ex,0}^+)(\boldsymbol{x}_{ex,0} - \hat{\boldsymbol{x}}_{ex,0}^+)^T] = \begin{bmatrix} \boldsymbol{P}_0 & 0 & 0 \\ 0 & \boldsymbol{\Sigma}_w & 0 \\ 0 & 0 & \boldsymbol{\Sigma}_v \end{bmatrix}$$

Recursive Computation:

$$\chi_0 = \mathrm{E}[\boldsymbol{x}]$$

$$\chi_i = \mathrm{E}[\boldsymbol{x}] + (\sqrt{(n+\lambda)\boldsymbol{P}_{xx}})_i, \quad i = 1, \ \ldots, \ n$$

$$\chi_i = \mathrm{E}[\boldsymbol{x}] - (\sqrt{(n+\lambda)\boldsymbol{P}_{xx}})_i, \quad i = n+1, \ \ldots, \ 2n$$

$$\chi_i^x(k+1|k) = f\left[\chi_i^x(k|k), \quad \boldsymbol{u}_k, \quad \chi_i^w(k)\right]$$

$$\hat{\boldsymbol{x}}_{k+1}^- = \hat{\boldsymbol{x}}(k+1|k) = \sum_{i=1}^{L} W_i^m \chi_i^x(k+1|k)$$

$$\boldsymbol{P}_k^- = \boldsymbol{P}(k+1|k) = \sum_{i=1}^{L} W_i^c [(\chi_i^x(k+1|k) - \hat{\boldsymbol{x}}_{k+1}^-)(\chi_i^x(k+1|k) - \hat{\boldsymbol{x}}_{k+1}^-)^T]$$

$$y_i(k+1|k) = g\left[\chi_i^x(k+1|k), \quad \boldsymbol{u}_k, \quad \boldsymbol{v}_k\right]$$

$$\hat{\boldsymbol{y}}_k = \sum_{i=1}^{L} W_i^m y_i(k+1|k)$$

$$\boldsymbol{P}_{yy}(k+1|k) = \sum_{i=1}^{L} W_i^c [(y_i(k+1|k) - \hat{\boldsymbol{y}}_k)(y_i(k+1|k) - \hat{\boldsymbol{y}}_k)^T]$$

$$\boldsymbol{P}_{xy}(k+1|k) = \sum_{i=1}^{L} W_i^c [(\chi_i^x(k+1|k) - \hat{\boldsymbol{x}}_{k+1}^-)(y_i(k+1|k) - \hat{\boldsymbol{y}}_k)^T]$$

$$\boldsymbol{L}_{k+1} = \boldsymbol{P}_{xy}(k+1|k) / \boldsymbol{P}_{yy}(k+1|k)$$

$$\hat{\boldsymbol{x}}_{k+1}^+ = \hat{\boldsymbol{x}}_{k+1}^- + \boldsymbol{L}_{k+1}(\boldsymbol{y}_k - \hat{\boldsymbol{y}}_k)$$

$$\boldsymbol{P}_k^+ = \boldsymbol{P}(k+1|k+1) = \boldsymbol{P}_k^- + \boldsymbol{L}_{k+1}\boldsymbol{P}_{yy}(k+1|k)\boldsymbol{L}_{k+1}^T$$

Efficient Square-root Implementation

The most computationally expensive operation in the UKF corresponds to calculating the new set of sigma points at each time update. This requires taking a matrix square-root of the state covariance matrix, $\mathbf{P} \in \mathbf{R}^{L \times L}$, given by $\mathbf{S}\mathbf{S}^T \in \mathbf{P}$. An efficient implementation using a Cholesky factorization requires in general $o(L^3/6)$ computations. While the square-root of $\mathbf{P}$ is an integral part of UKF, it is still the full covariance $\mathbf{P}$ which is recursively updated. In the square-root UKF implementation, $\mathbf{S}$ will be propagated

directly, avoiding the need to re-factorize at each time step. The algorithm will in general still be $o(L^3)$, but with improved numerical properties similar to those of standard square-root Kalman filters.

The square-root form of the UKF makes use of three powerful linear algebra techniques, QR decomposition, Cholesky factor updating and efficient least squares. The complete specification of the a square-root unscented Kalman filter (SR-UKF) is listed in Table 2.

Table 2. Summary of the SR-UKF Algorithm

Initialization：

$$k = 0$$

$$\hat{\boldsymbol{x}}_0^+ = E(\boldsymbol{x}_0)$$

$$\boldsymbol{S}_0 = chol\{\mathrm{E}[(\boldsymbol{x}_0 - \hat{\boldsymbol{x}}_0^+)(\boldsymbol{x}_0 - \hat{\boldsymbol{x}}_0^+)^T]\}$$

Recursive Computation：

$$\chi_{k-1} = \{\hat{\boldsymbol{x}}_{k-1}^+, \hat{\boldsymbol{x}}_{k-1}^+ + \eta \boldsymbol{S}_{k-1}, \hat{\boldsymbol{x}}_{k-1}^+ - \eta \boldsymbol{S}_{k-1}\}$$

$$\hat{\chi}_k^- = f(\chi_{k-1}, \boldsymbol{u}_{k-1})$$

$$\hat{\boldsymbol{x}}_k^- = \sum_{i=1}^{L} W_i^m \hat{\chi}_{i,k}^-$$

$$\boldsymbol{S}_k^- = qr\left\{\left[\sqrt{W_1^c}(\hat{\chi}_{12L,k}^- - \hat{\boldsymbol{x}}_k^-) \quad \sqrt{\boldsymbol{\Sigma}_w}\right]\right\}$$

$$\boldsymbol{S}_k^- = cholupdate\{\boldsymbol{S}_k^-, \quad \sqrt{abs(W_0^c)}(\hat{\chi}_{0,k}^- - \hat{\boldsymbol{x}}_k^-), \quad \mathrm{sgn}(W_0^c)\}$$

$$y_k = g\left[\hat{\chi}_k^-, \quad \boldsymbol{u}_k\right]$$

$$\hat{\boldsymbol{y}}_k = \sum_{i=1}^{L} W_i^m y_{i,k}$$

$$\boldsymbol{S}_{yk}^- = qr\left\{\left[\sqrt{W_1^c}(y_{i,k} - \hat{\boldsymbol{y}}_k) \quad \sqrt{\boldsymbol{\Sigma}_v}\right]\right\}$$

$$\boldsymbol{S}_{yk}^- = cholupdate\left\{\boldsymbol{S}_{yk}^-, \quad \sqrt{abs(W_0^c)}(y_{0,k} - \hat{\boldsymbol{y}}_k), \quad \mathrm{sgn}(W_0^c)\right\}$$

$$\boldsymbol{P}_{xy,k} = \sum_{i=1}^{L} W_i^c[(\chi_{k-1} - \hat{\boldsymbol{x}}_{k+1}^-)(y_k - \hat{\boldsymbol{y}}_k)^T]$$

$$\boldsymbol{L}_k = (\boldsymbol{P}_{xy,k}\boldsymbol{S}_{yk}^{-T})/\boldsymbol{S}_{yk}^-$$

$$\hat{\boldsymbol{x}}_k^+ = \hat{\boldsymbol{x}}_k^- + \boldsymbol{L}_k(\boldsymbol{y} - \hat{\boldsymbol{y}}_k)$$

$$\boldsymbol{U} = \boldsymbol{L}_k\boldsymbol{S}_{yk}^-$$

$$\boldsymbol{S}_k = cholupdate\left\{\boldsymbol{S}_{yk}^-, \quad \boldsymbol{U}, \quad -1\right\}$$

UKF-based SOC Estimator

There are totally 3 states in the proposed battery model, so, when designing the UKF-based SOC estimator, the key factors are set with $L = 3$, $\beta = 2$ and $\alpha^2 = 0.0003$, then $\eta = \sqrt{L+\lambda} = \sqrt{L + \alpha^2(L+\kappa) - L} = \sqrt{\alpha^2(L+\kappa)}$.

When the filter is used for state estimation, κ =0, so $\eta = \sqrt{\alpha^2 L} = \sqrt{0.0003 \times 3} = 0.03$,

$\lambda = \alpha^2(L+\kappa) - L = L(\alpha^2 - 1) = 3 \times (0.0003 - 1) = -2.9991$.

The weight factors are set to

$$W_0^m = \frac{\lambda}{L+\lambda} = \frac{\alpha^2(L+\kappa) - L}{L + \alpha^2(L+\kappa) - L} = \frac{\alpha^2(L+\kappa) - L}{\alpha^2(L+\kappa)}$$

$$= 1 - \frac{L}{\alpha^2(L+\kappa)} = 1 - \frac{1}{0.0003},$$

$$W_0^c = \frac{\lambda}{L+\lambda} + (1 - \alpha^2 + \beta) = W_0^m + (1 - 0.0003 + 2) = 3.9997 - \frac{1}{0.0003},$$

and

$$W_i^m = W_i^c = \frac{1}{2(L+\lambda)} = \frac{1}{2 \times (\alpha^2(L+\kappa))} = \frac{1}{0.0018}.$$

By using the square-root UKF listed in Table 2, and with the key factors set above, the UKF -based SOC estimator is achieved.

Implementation of the Estimator on DSP

The adaptive SOC estimator based on UKF was implemented on a DSP (Digital Signal Processor) based platform by an efficient method. The platform uses a TMS320F2808 released by Texas Instrument (TI®) as its main processor, which is a 32-bit fix-point DSP processor. The method utilized the high-performance algorithm units, the parallel computing and the pipeline architecture of the DSP to get a high efficient result. Due to the parallel structure, several sharing buffers were applied to make the several parts operation in the right order.

Due to the floating point operation of the algorithm, and for a high calculation efficiency, all the addition and subtraction were designed and converted to be the fix-point type, which is realized based on the a point-calibration method. The multiplication operation was designed based on the hardware multiplexer embedded in the DSP chip.

The testing software was developed by using the Matlab/Simulink® and Embedded Target for Texas Instrument (TI ®) C2000 toolbox. To get a high efficiency, the core algorithm is programmed with a s-Function in C language. In the designed s-Funciton, the SOC, the voltage on R_1C_1 circuit and R_2C_2 circuit, and the covariance matrices, which needs to be propagated at each step are set to be the states, and current, voltage are set to be the input and output of the model respectively. The s-Function was integrated into the SOC estimator, and by the automatic code generation of the Matlab ®, we at last get the c-code for the DSP, and by the compiling and downloading with CCS® (Code Composer Studio), we can test our SOC estimator running on the DSP platform. The integrated SOC estimator model was shown in Fig. 6.

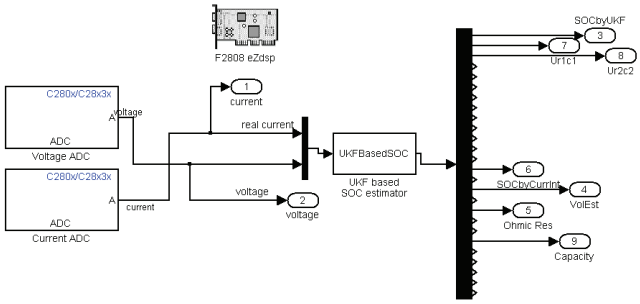

Fig.6. Integrated SOC estimator model in Matlab/Simulink®

Experiment and Analysis

Experimental Setup

As shown in Fig.7., the experimental setup consisted of a Battery Testing System (BTS, could be Arbin® or Digatron® etc.), a battery management system, a CAN communication module (here we used a ZLG® USBCAN-II board), a monitor unit (usually could be a NI Labview® -based virtual measurement system by using a PC as its platform), a current Hall sensor (LEM® DHAB S18), an ambient chamber (Espec® PDR-4K) and the battery pack to be tested. The BTS was responsible for loading the battery based on the designed program with maximum voltage of 400V and maximum charging/discharging current up to 500A. The tested battery pack was composed with 96 LiMnO2-typed cells connected in series, with 8Ah as its nominal capacity.

The recorded signals included load current, terminal voltage, temperature, accumulative Amp-hour (Ah) and Watt-hour (Wh). During testing, the BMS also collected the voltage and current of the battery system. The load current was measured by the Hall current sensor, whose error is less than 0.5%. The terminal voltage measured by BMS was implemented by the voltage measurement circuit

designed embedded in BMS PCB board, and the voltage measurement error is less than 0.4%. The Labview® - based monitor unit was responsible for the real-time signal display and data store, it communicated with BMS through CAN bus, and for the real-time requirements, the baud-rate was set to be 500k.

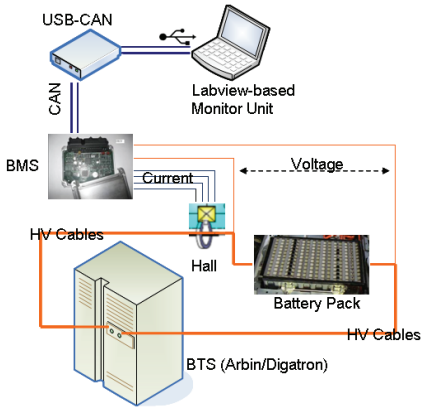

Fig.7. Experimental setup

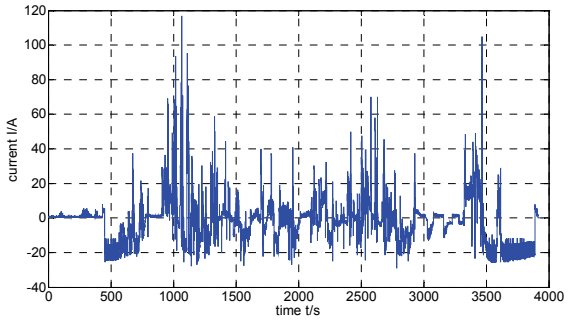

Fig.8. Current profile under on-road test

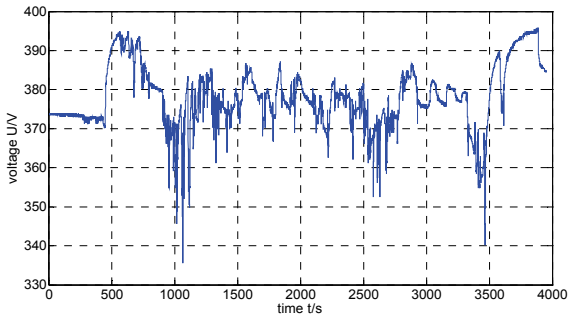

Fig.9. Voltage variation under on-road test

Two different tests were implemented to test the UKF-based SOC estimator. In the first test, the current load, Fig.8, was set to be the actual load during the vehicle tested on-road. Under this test, the voltage variation of the battery pack is shown in Fig9. In the second test, the current load, Fig.10, lasted for about 8000s, and was composed of 3 different sub-profiles, Fig.11, which caused a voltage variance of the battery pack as shown in Fig.12. First sub-profile of the second test started from the beginning to around 5500s, the second sub-profile started from 5500s to 6500s, and the third sub-profile started from 6500s to the last. Both testing current profiles are complicated enough to stimulate the dynamic characteristics of the battery pack, thus, we could evaluate the SOC estimator more confidently.

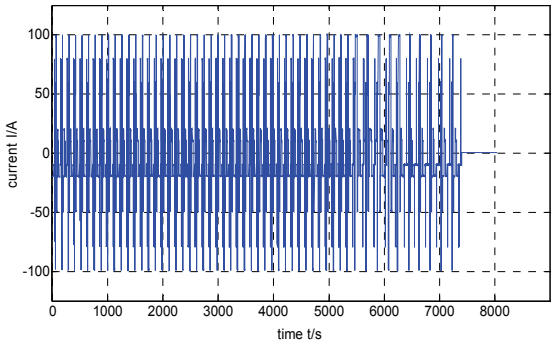

Fig.10. Testing current profiles

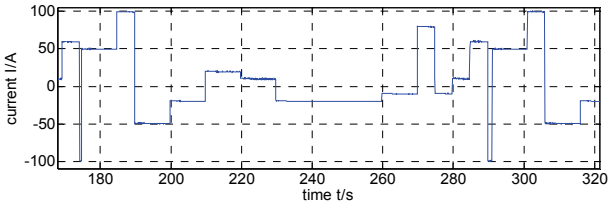

(a) First sub-profile

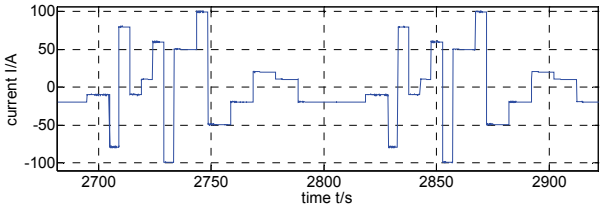

(b) Second sub-profile

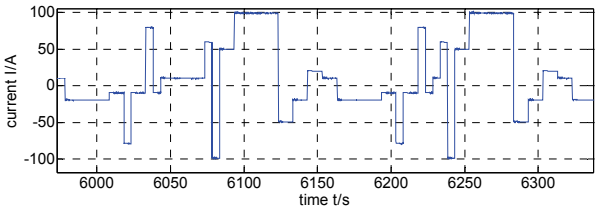

(c) Third sub-profile

Fig.11. Sub-profiles of the testing current

Results Analysis

Results of the SOC estimator based on UKF under the two test cases discussed above are shown in Fig.13 – Fig.16. Both the SOC estimation and the SOC error are plotted in those figures. This amplifies the details between the two estimators.

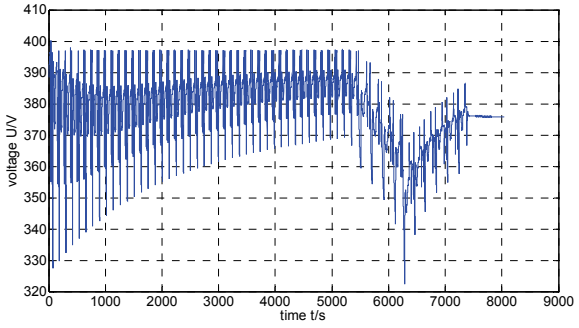

Fig.12. Voltage variation under testing current

In the first case, initial value of SOC for UKF-based estimator is set to be 65%, while the true SOC is 44%,

which is got according to the co-relationship of SOC and OCV, as shown in Fig.2. Similarly, in the second test case, initial value of SOC for UKF-based estimator is set to be 70%, while the true value is 56%. By this setup, we can investigate the convergence of the estimators, and to see if the estimator is sensitive to the initial value.

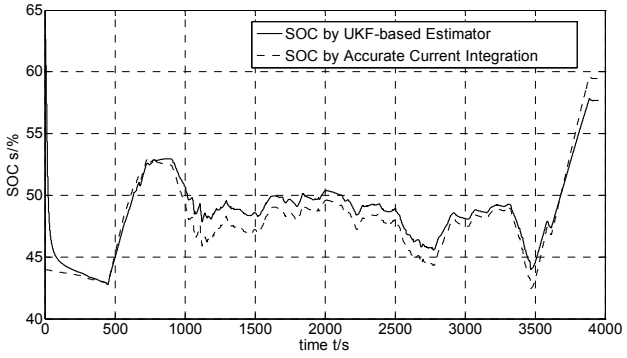

Fig.13. SOC variation under on-road test

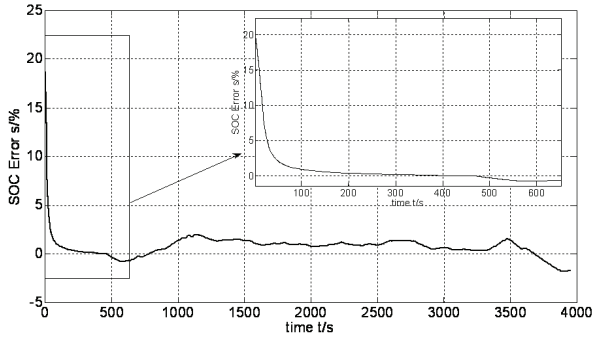

Fig.14. SOC estimation error under on-road test

We first discuss the results of the first test case. Fig. 13 shows the SOC estimation for this test based on UKF. And the associated estimation errors are shown in Fig.14. It is clear that, once converging, the UKF-based SOC estimator can estimate the battery SOC accurately, with a maximum estimation error less than 3%.

In the second test case, the SOC estimation based on UKF is shown in Fig.15, and the associated estimation errors are shown in Fig.16. Likewise, we can see the good performance of the UKF-based SOC estimator, the maximum estimation error is less than 4.5%.

In both cases, we can also find that the UKF-based SOC estimator can compensate the initial SOC errors quickly and accurately track the true SOC values. From Fig.14 and Fig.16, it is clear to see that the errors in both test cases can converge into a $\pm$4.5% error band in less than 100s.

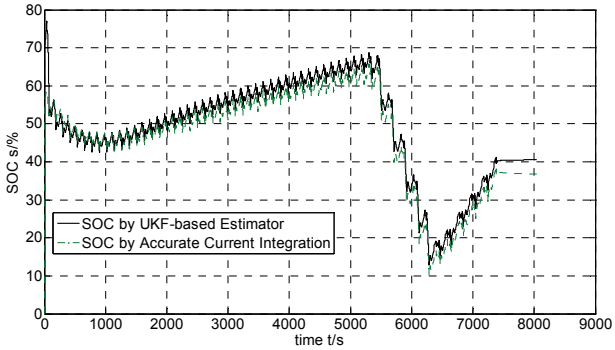

Fig.15. SOC variation under testing current

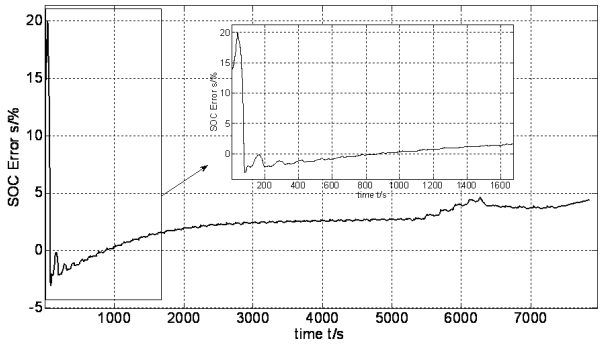

Fig.16. SOC estimation error under testing current

A Comparison with EKF-based SOC Estimator

To demonstrate that the UKF-based SOC estimator outperforms the EKF-based SOC estimator, we here show how the two different SOC estimators perform under a same testing condition. We here use the second test profile as the example, as shown in Fig.10 and Fig.11. The two estimators are set with the same initial conditions.

Fig. 17 shows the UKF-based and EKF-based SOC estimation results under the test, and Fig. 18 shows the error of the estimation. Note that, in this comparison, the two estimators are all set with the initial SOC 70%.

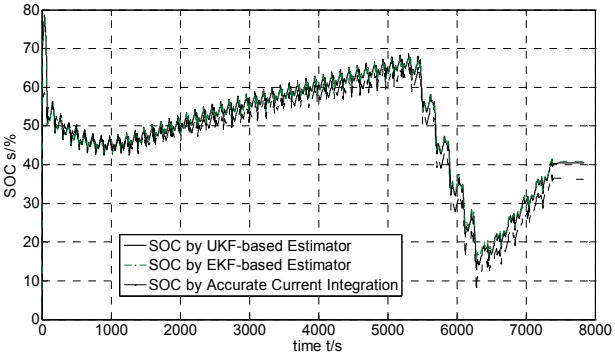

Fig.17. SOC estimation of different estimators

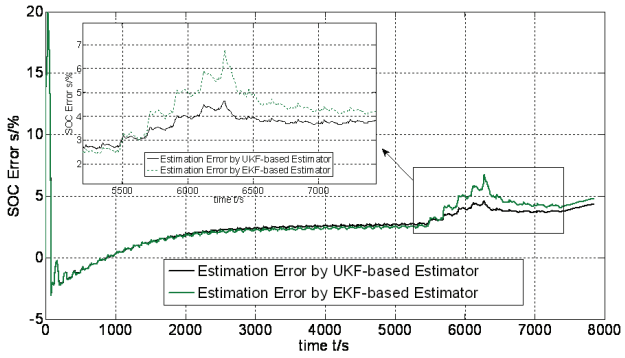

Fig.18. SOC estimation error of UKF- and EKF-based estimators

From Fig. 17 and Fig. 18, we can find that the UKF-based SOC estimator does outperform the EKF-based SOC estimator, although the performance improvement is not significant. Possible reasons may be that the linearity of the OCV in the SOC range (10% to 50%) during this test is relatively good, as shown in Fig.2. The maximum difference is about 2%. The most significant difference between the two estimators is enlarged in Fig.18, which happens between SOC 20% and SOC 10%. This relatively large difference is caused by the nonlinearity of the OCV and

SOC relationship. From Fig.2, we can see that, when SOC goes between 20% and 10%, the slope of the curve changes a lot. This could be seen as a collaborative evidence of the enhancement of UKF to EKF in dealing with the nonlinearity system state estimation.

Conclusions

This paper describes a UKF-based SOC estimator for the LiMnO2 batteries used on EVs or HEVs. The method was illustrated by modeling the dynamic behavior of the battery based on an equivalent circuit, composed of 3 resistors, 2 capacitors and a voltage source. This model can represent the dynamic characteristics of the battery very closely and does not increase the calculation complexity. The application of UKF, with its inherent predictor-corrector mechanism, in SOC estimation was shown to be robust, and especially, compared with EKF-based estimator, more accurately to deal with the state estimation of non-linear system. Meanwhile, the UKF-based SOC estimator has almost the same computation complexity with EKF-based SOC estimator, which makes the UKF-based estimator more competitive. To enhance the efficiency and reduce the calculation cost, the SOC estimator was last designed with a SR-UKF, and the experimental results show that the SR-UKF based SOC estimator can estimate the battery SOC accurately and it outperforms the EKF-based estimator, especially when the battery was cycled with the SOC between 10% and 20%, where the nonlinearity of the co-relationship of SOC and OCV is most significant .

Acknowledgment

The authors would like to express deep gratitude to the colleagues, who are Dr. Wang J.Y, Dr. Gu W.J et al. for their help in the experiments and helpful discussions and suggestions. This work is financially supported by the Doctoral Fund of Ministry of Education of China (RFDP) under Grant No. 20100072120026. It is also funded by Science and Technology Planning Project of Shanghai under Grant No. 09dz2201400.

REFERENCES

[1] S. Piller, M. Perrin, A. Jossen. “Methods for state-of-charge determination and their applications”. Journal of Power Sources, vol. 96, pp113-120, 2001.

[2] G. O. Patillon and J. N. d’ Alché-Buc, “Neural network adaptive modeling of battery discharge behavior.” Artificial Neural Networks ICANN’ 97 7th Int. Conf., vol. 1327, pp 1095-1100, 1997.

[3] S. R. Bhatikar, R. L. Mahajan, K. Wipke, and V. Johnson. (1999, Aug.) “Neural network based energy storage system modeling for hybrid electric vehicles”. Nat. Renewable Energy Lab., Golden, CO. [Online] www.Ctts.Nrel.Gov/analysis/reading_room.

[4] Chan CC, Lo EWC, Shen W. “The available capacity computation model based on artificial neural network for lead-acid batteries in electric vehicles”. Journal of Power Sources, vol. 87, pp201-204, 2000.

[5] Shen WX, Chan CC, Lo EWC, Chau KT. “A new batteyr available caoacity indicator for electric vehicles using neural network”. Energy Conversion and Management, vol. 43, pp 817-826, 2002.

[6] Shen WX. “State of available capacity estimation for lead-acid batteries in electric vehicles using neural network”. Energy Conversion and Management, vol. 48, pp433-442, 2007.

[7] Shen WX, Chau KT, Chan CC. “Neural network-based residual capacity indicator for nickel-metal hydride batteries in electric vehicles”. IEEE Transaction on Vehicular Technology, vol. 54, pp1705-1712, 2005.

[8] Morita Y, Yamamoto S, Lee SH, Mizuno N. “On-line detection of state-of-charge in lead acid battery using radial basis function neural network”. Asia Journal of Control, vol. 8, pp268-273, 2006.

[9] Cheng B, Bai ZF, Cao BG. “State of charge estimation based on evolutionary neural network”. Energy Conversion and Management, vol. 49, pp2788-2794, 2008.

[10] Cheng B. Zhou YL, Zhang JX, Wang JP, Cao BG. “Ni-MH batteries state-of-charge prediction based on immune evolutionary network”. Energy Conversion and Management, vol. 50, pp3078-3086, 2009.

[11] Salkind AJ, Fennie C, Singh P, Atwater T, Reisne DE. “Determination of state-of-charge and state-of-health of batteries by fuzzy logic methodology”. Journal of Power Sources, vol 80, pp293-300, 1999.

[12] Chau KT, Wu KC, Chan CC. “A new battery capacity indicator for nickel-metal hydride battery powered electric vehicles using adaptive neuro-fuzzy inference system”. Energy Conversion and Management, vol. 44, pp2059-2071, 2003.

[13] Malkhandi S. “Fuzzy logic- based learning system and estimation of state of charge of lead-acid battery”. Engineering Applications of Artificial Intelligence, vol. 19, pp479-485, 2006.

[14] Hansen T, Wang CJ. “Support vector based battery state of charge estimator”. Journal of Power Sources, vol.141, pp351-358, 2005.

[15] Shi QS, Zhang CH, Cui NX. “Estimation of battery state-of-charge using v-support vector regression algorithm”. International Journal of Automotive Technology, vol. 9, pp 759-764, 2008.

[16] Hu XS, Sun FC. “Fuzzy clustering based multi-model support vector regression state of charge estimator for lithium-ion battery of electric vehicle”. International Conference on Intelligence Human-Machine Systems and Cybernetics, pp392-396, 2009.

[17] G. Plett. “Extended kalman filtering for battery management systems of LiPB-based HEV battery packs. Part 2. Modeling and identification”. Journal of Power Sources, vol. 134, pp262-276, 2004.

[18] G. Plett. “Extended kalman filtering for battery management systems of LiPB-based HEV battery packs. Part 3. State and parameter estimation”. Journal of Power Sources, vol. 134, pp277-292, 2004.

[19] Dai H.F., Wei X.Z., Sun Z.C. “Model Based SOC Estimation for High-power Li-ion Battery Packs Used on FCHVs”. High Technology Letters, vol. 13, pp322-326, 2007.

[20] Dai H.F., Wei X.Z., Sun Z.C. “Estimate state of charge of power lithium-ion batteries used on fuel cell hybrid vehicle with method based on extended Kalman filtering”. Chinese Journal of Mechanical Engineering, vol. 43, pp92-95, 2007.

[21] Plett GL. “Sigma-point Kalman filtering for battery management systems of LiPB-based HEV battery packs- Part 1: introduction and state estimation, Part 2: simultaneous state and parameter estimation”. Journal of Power Sources, vol. 161, pp1356-1384, 2006.

[22] Santhanagopalan S, White RE. “State of charge estimation using an unscented filter for high power lithium ion cells”. International Journal of Energy Research, vol. 34, pp52-163, 2010.

[23] Han JY, Kim DC, Sunwoo M. “State-of-charge estimation of lead-acid batteries using an adaptive extended Kalman filter”. Journal of Power Sources, vol. 188, pp606-612, 2009.

[24] Chen Quanshi, Lin Chengtao, “Summarization of Studies on Performance models of batteries for electric vehicle”. Automobile Technology, vol. 3, pp1-5, 2005.

[25] Wei Xuezhe, Zou Guangnan, Sun Zechang, “Modeling and parameter estimation of Li-ion battery in a fuel cell vehicle”. Chinese Journal of Power Sources, vol. 28, pp605-608, 2004.

[26] Wan EA, Van Der Merwe R. “The unscented Kalman filter for nonlinear estimation”. IEEE Symposium on Adaptive Systems for Signal Processing, Communications and Control, pp153-158, 2000.

[27] Van Der Merwe R. “Sigma-point Kalman filters for probabilistic inference in dynamic state-space models”. Dissertation for the Degree of Doctor of Philosophy. Oregon Health & Science University. Portland, USA, 2004.

***Authors**: dr Haifeng Dai, School of Automotive Studies, Tongji University, Shanghai 201804, China, E-mail: tongjidai@gmail.com.*